Journal of Manufacturing Processes 59 (2020) 523–534

Contents lists available at ScienceDirect

Journal of Manufacturing Processes

journal homepage: www.elsevier.com/locate/manpro

On the role of wet abrasive centrifugal barrel finishing on surface enhancement and material removal rate of LPBF stainless steel 316L

Mahyar Khorasani [a,b,*], Ian Gibson [a,b], AmirHossein Ghasemi [c], Milan Brandt [d], Martin Leary [d]

[a] School of Engineering, Deakin University, Waurn Ponds, Victoria, Australia
[b] Fraunhofer Centre for Complex System Engineering, Department of Design, Production and Management, University of Twente, Enschede, the Netherlands
[c] Faculty of Engineering, University of Kashan, Ravandi Bolivar, Kashan, Iran
[d] School of Engineering, RMIT University, Victoria, Australia

ARTICLE INFO

Keywords:
Abrasive centrifugal barrel finishing
Additive manufacturing
Selective laser melting
Surface roughness

ABSTRACT

Poor surface finish is a primary challenge to the commercial implementation of Additive Manufacturing (AM). To solve this problem, various Material Removal Rate (MRR) processes have been proposed. However, current methods provide sub-optimal outcomes for the complex geometry enabled by AM. Abrasive Centrifugal Barrel Finishing (ACBF) and Wet Abrasive Centrifugal Barrel Finishing (WACBF) can provide an effective surface finishing solution method that is compatible with the geometric complexity of AM components. ACBF and WACBF are commercially robust processes that can economically process multiple components to polish cavities and intricate internal geometry. This research documents the experimental application of WACBF to polish Stainless Steel (SS) 316 L, printed by Laser-Based Powder Bed Fusion (LPBF). The performance of WACBF on volumetric MRR is also examined. To assess the homogeneity of the abrasive process, surface roughness was quantified in directions parallel, vertical and at 45° to the laser scan direction. A Taguchi L8 experiment was devised with three repetitions to assess the influence of WACBF parameters including rotational speed, media size and running time on the measured surface roughness and material removal rate. This experiment confirms that surface roughness and MRR have a non-linear correlation with increasing the rotational speed, and that enhanced surface roughness is achieved with larger media size. An important observation for commercial implementation is that increasing the time of the process provides an insignificant reduction in surface quality, and MRR implying that for commercial applications, high-throughput can be achieved without compromising quality. These experiments confirm that WACBF processing improved the surface roughness for parallel, vertical and 45° surfaces by 62.30 %, 56.33 %, and 56.08 % respectively.

1. Introduction

Additive Manufacturing (AM) provides numerous technical and economic opportunities in comparison to traditional manufacturing processes: lower material wastage, direct digital design with no custom tooling, high geometric freedom with fewer manufacturing constraints and the opportunity to fabricate highly integrated net shapes with little post-processing and assembly [1–3]. However, technical challenges still exist in the commercial application AM systems like Laser-Based Powder Bed Fusion (LPBF) is a potential for relatively high dimensional variation and poor surface finish [4–6].

Traditional methods exist to enhance the surface finish of AM components, for example, glass bead blasting, conventional milling, Electrical Discharge Machining (EDM) and surface grinding. These methods have some critical disadvantages, specifically for the complex geometries common to high-complexity AM components. Khorasani et al. [7] investigated the milling of Ti6Al4V specimens produced by LPBF where CNC milling was applied and tool deflection was characterized according to specific machining parameters. Results showed that deflection affects the roughness and geometrical tolerance of manufactured component [7]. Khorasani et al. [8] also investigated the effects of machining parameter, tool path and heat treatment on the surface roughness of LPBF components using ANN to determine, predict and optimize surface roughness. To enhance the surface quality of LPBF parts, they suggested to design appropriate tool paths, and cutting parameters with lower scallop height, finishing allowance and higher spindle speed and annealing temperature. EDM and bead blasting

* Corresponding author.
E-mail addresses: a.khorasani@deakin.edu.au (M. Khorasani), i.gibson@utwente.nl (I. Gibson), amir_hosein_ghasemi2012@yahoo.com (A. Ghasemi), milan.brandt@rmit.edu.au (M. Brandt), martin.leary@rmit.edu.au (M. Leary).

https://doi.org/10.1016/j.jmapro.2020.09.058
Received 28 November 2019; Received in revised form 7 August 2020; Accepted 26 September 2020
Available online 14 October 2020
1526-6125/© 2020 The Author(s). Published by Elsevier Ltd on behalf of The Society of Manufacturing Engineers. This is an open access article under the CC BY license (http://creativecommons.org/licenses/by/4.0/).

Nomenclature

ACBF	Abrasive Centrifugal Barrel Finishing
ABS	Acrylonitrile Butadiene Styrene
AJM	Abrasive Jet Machining
AM	Additive Manufacturing
AWJM	Abrasive Water Jet Machining
EBM	Electron Beam Melting
EDM	Electron Discharge Machining
LAEBI	Large Area Electron Beam Irradiation
MANOVA	Multivariate Analysis of Variance
MRR	Material removal rate
MRRv	Volumetric material removal
OEM	Original Equipment Manufacturer
PBF	Powder Bed Fusion
PTEF	Polytetrafluoroethylene
P-value	Probability Values
R^2	Coefficient of Determination
S/N	Signal-to-Noise Ratio
SLM	Selective Laser Melting
SLS	Selective Laser Sinterin
SS	Stainless Steel
WACBF	Wet Abrasive Centrifugal Finishing
$X_{(i)}$	Independent(S) Variable (Input)
$Y_{(i)}$	Dependent Variable (Output)

performed poorly in the enhancement of surface roughness, while electron beam glazing is feasible for flat surfaces and provided the flat surface with fine-grained microstructure. Lober et al. [10] investigated various mechanical processes for surface finishing of LPBF Stainless steel 316 L components, such as grinding, electrolytic etching, sandblasting and plasma polishing. Of these methods, grinding provided the best outcomes to enhance surface quality (surface roughness (R_a) reduced from 15 μm to 0.34 μm), but this method is only compatible with regular planar geometry, and is therefore incompatible with the commercial requirements of AM surface finishing. Rossi et al. [11] showed they were able to reduce surface roughness of a horizontal plane from 12.01 μm to 4.00 μm for LPBF iron–nickel–copper-based components. On the vertical plane, they could reduce 15.00 μm (for as-built) to 12.00 μm. Surface roughness can be further decreased through the application of Polytetrafluoroethylene-based (PTFE) coatings, also enhancing surface corrosion resistance. Beaucamp et al. [12] developed a new shape adaptive grinding tool that has achieved a surface finish of up to 10 nm in components manufactured by EBM and LPBF but it is not compatible with very complex geometry and captive components also cannot be machined. Lamikiz et al. [13] applied laser irradiation for polishing LPBF and Selective Laser Sintering (SLS) components. In this process, the upper microscopic layer of the manufactured components was locally melted by the laser energy source. This melt-pool rapidly re-solidified under the protection of shielding gas, resulting in locally enhanced surface roughness in the order of 80 % with no heat-affected zones or cracking observed. This method has been successfully demonstrated on inclined plane surfaces. Meanwhile, Uno et al. [14] worked on the surface finishing of metallic molds through a novel process known as Large Area Electron Beam Irradiation (LAEBI). In this process, an unfocused, high energy electron beam is applied with a diameter of up to 60 mm. Unlike laser irradiation, the material is not re-solidified but is locally vaporized, making this process potentially faster than competing methods. LAEBI has been demonstrated to decrease surface roughness from 6 μm to 1 μm. Moreover, this process also improved the corrosion resistance of the specimens.

These technologies are generally only suitable for external component surfaces that have low geometric complexity. Furthermore, machining processes are serial and can process only one component at a time. To overcome these limitations, WACBF or Abrasive Jet Machining (AJM) and Abrasive Water Jet Machining (AWJM) provide an emerging opportunity for improving surface roughness of geometrically complex high-value AM products. Furthermore, WACBF provides relevant production advantages including the avoidance of clamping fixtures, requires no complex tool path planning, and is compatible with small production batches. Boschato et al. [18] worked on centrifugal barrel finishing by changing the rotational speed of the process (around 100 rpm and higher) for complex components. They found that with process times of 10 h the surface quality improved. However, no significant change was observed by further increasing the process time to 50 h. Nalli et al. [19] investigated the effect of fabrication process parameter and centrifugal barrel finishing speed on dimensions and tensile behaviour of Ti-6Al-4 V components. This research showed that an increase in rotational speed improves roughness and surface quality. Lesyk et al. [20] compared shot peening and barrel finishing of Inconel 718 components. They found that surface finish and surface waviness improved by barrel finishing, while shot penning improved mechanical properties. In shot peening, mechanical work induced on the surface of the samples leads to a decrease in micro and macro defects. Lesyk et al. [21] also compared shot peening, barrel finishing, ultra-sonic shot peening and ultra-sonic impact treatment for post-processing of Inconel 718 components. The results showed that barrel finishing induced less residual stress compared to other treatments. Na et al. [22] studied the effect of time and speed in barrel finishing on the roughness of stainless steel components. The findings showed that at 60 rpm and after 40 min of finishing the value of roughness decreased by 70 % with no significant improvement for longer times. In the case of 80 and 100 rpm, this improvement was achieved in 30 min of processing. Singh et al. [23] studied chemical assisted magnetic abrasive finishing of tubes made of Inconel 625. The investigated factors were process time, rotational speed, abrasive size, amount of abrasive and chemical agent on the surface roughness and MRR. They found that process time and media size were the most influential parameters followed by amount of abrasive particles, rotational speed and chemical agent. Ferchow et al. [24] used abrasive flow machining to polish internal surfaces of tubes made by LPBF. This work showed an acceptable deviation between the proposed rheological model and the measurement of down-skin and up-skin for material removal thickness.

Most of the current literature is related to the using conventional machining for post-processing of AM parts and no report was found based on using WACBF for AM components.

In this research, Taguchi Design of Experiment (DOE) was selected to experimentally characterize the effect of WACBF process parameters on the MRR and surface finish of LPBF specimens. Industrially, relevant WACBF control factors were selected and associated surface roughness was characterized in multiple directions to the laser scan direction. These measurements were acquired with multiple repetitions to ensure statistically robust outcomes. The effects of each control factor and associated interactions with surface roughness and MRR are characterized by appropriate regression models and the commercial implications of these outcomes are discussed.

2. Experimental setup

2.1. Design of experiment

The relevant control factors for commercial WACBF systems are media size, rotational speed and processing time. A Taguchi L8 Design of Experiment was selected with three repetitions as it allows the effect of

Table 1
Design of experiment.

Number of repetitions	Test Number	Media size	Rotational Speed (Rpm)	Time (min)
3	1	3 × 3	100	200
3	2	6 × 6	100	240
3	3	3 × 3	120	200
3	4	6 × 6	120	240
3	5	6 × 6	140	200
3	6	3 × 3	140	240
3	7	6 × 6	160	200
3	8	3 × 3	160	240

Table 2
Machine build process parameters.

System Parameters	Value
Min. Scan Line / Wall Thickness	120 μm
Operational Beam Focus Variable	100 μm
Layer Thickness	30 μm
Laser Power	175W
Hatch Space	120 μm
Scan Speed	560 mm/s
Laser spot diameter	0.2 mm

these control factors on surface roughness to be assessed for multiple levels within a relatively compact DOE (Table 1). Taguchi provides more flexibility for parameter levels in the same test number compared to factorial and RSM DOEs. Based on manufacturer recommendation, speed is the most important factor and since two different media sizes were used, Taguchi L8 meets the requirement of this experiment. For each run one component was fed to the barrel and fresh media was used for each new experimentation.

2.2. Powder material and SLM operation

Samples were manufactured with an SLM 125 H L system (SLM Solutions GmbH, Lubeck, Germany), equipped with YLR-Fiber laser. Samples were manufactured horizontally and the SLM processing parameters are typical commercial specifications (Table 2). The powder material was low carbon stainless steel (SS 316 L) and specimens were designed in the form of hexagonal geometry with 6.81 mm thickness. Fig. 1)(A) illustrates magnification of the powder and (B) illustrates examples of the samples manufactured in this study. Fig. 1(C) shows that the average particle distribution size used in this experiment was 35 μm.

2.3. Material removal rate

Material removal rate (MRR) was measured based on the volume of the samples. The measurements were taken using Mitotoyo micrometre

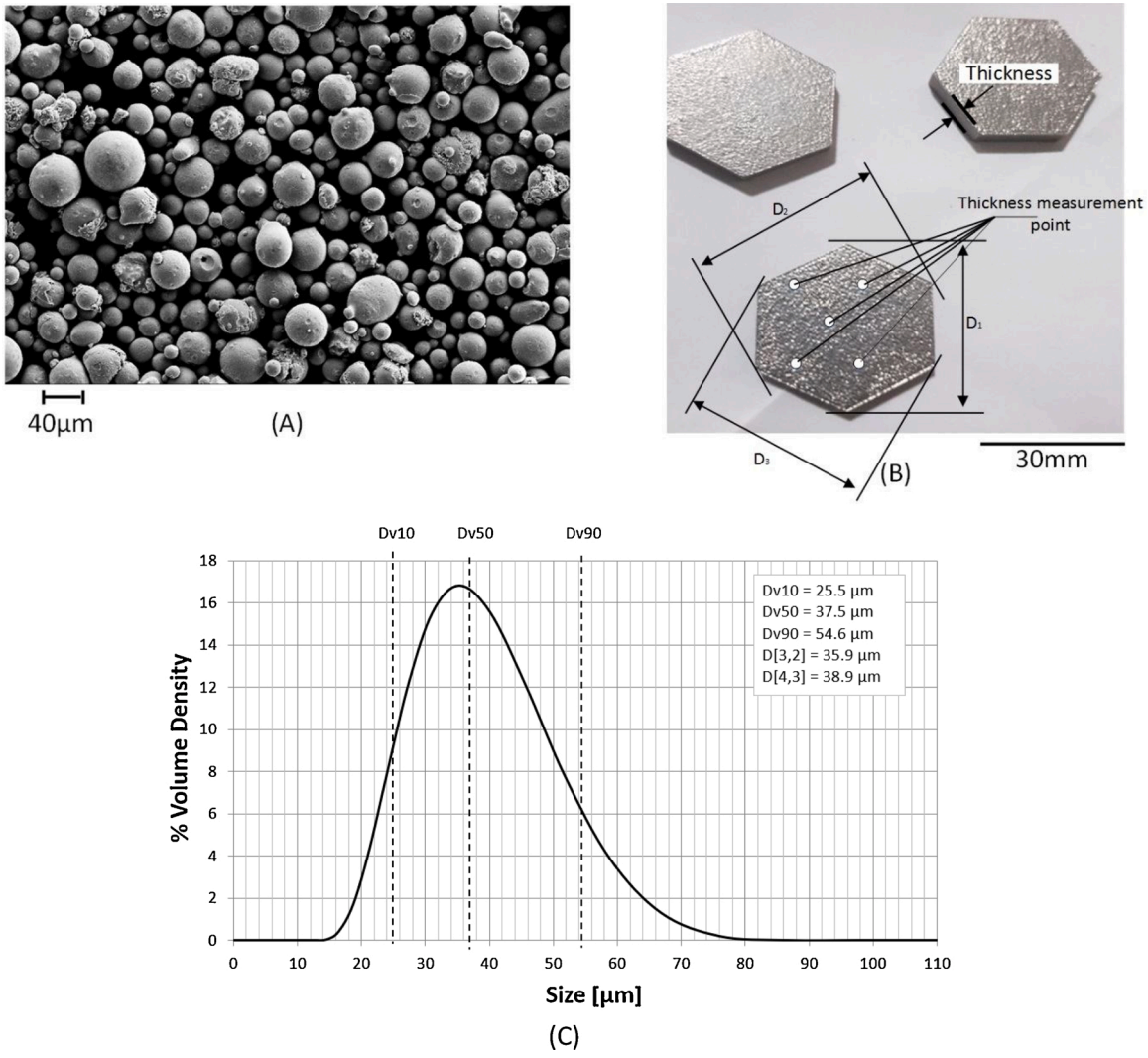

Fig. 1. (A) Powder (B) Printed samples and (C) powder volume density.

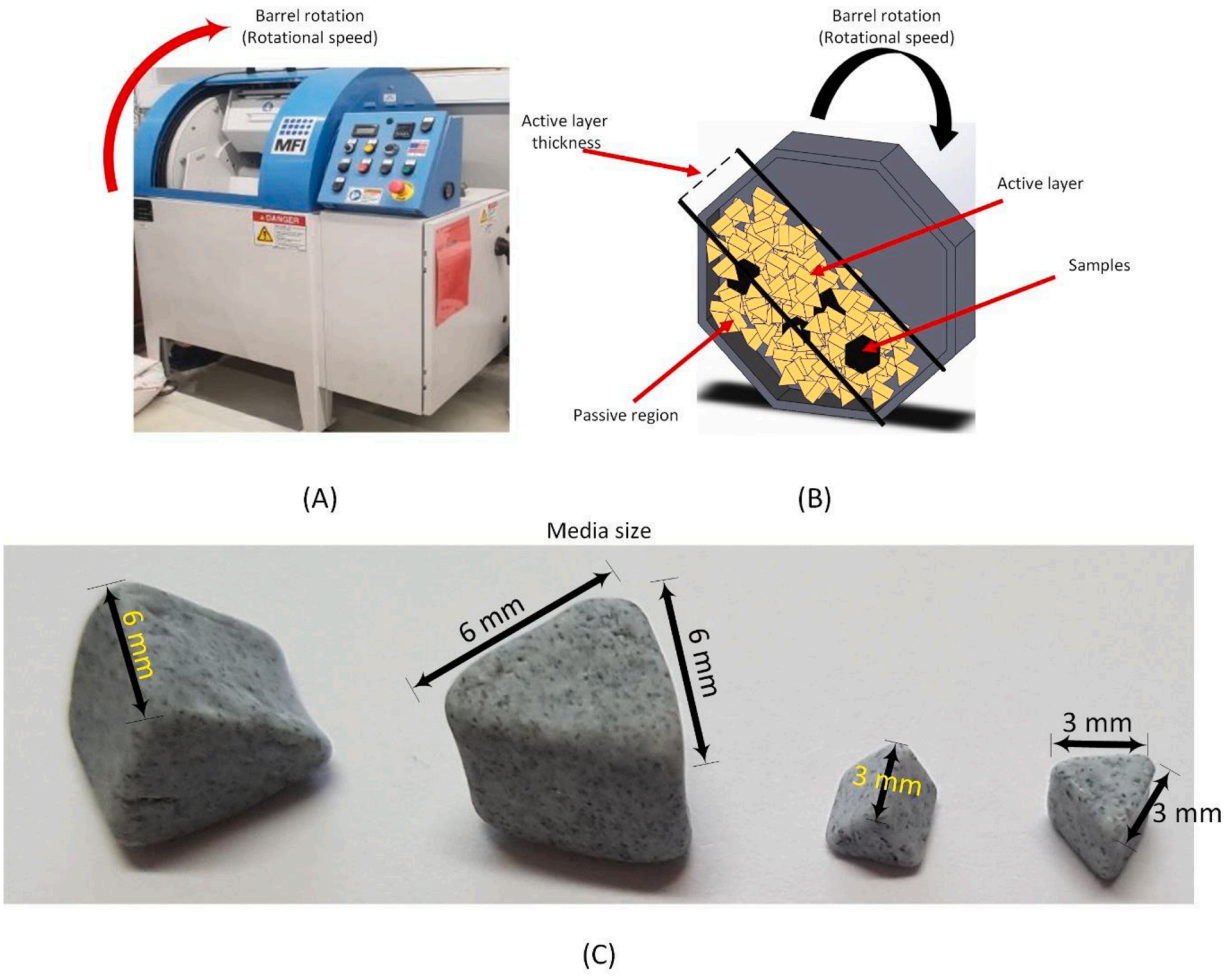

Fig. 2. (A) WACBF machine (B) Active and passive regions in WACBF (C) Media size.

at 20 °C and 30 % humidity to have maximum consistency for all measurements. Two types of Mitotoyo micrometre on fixed stand with 1 μm resolution and the total range of 0–25.00 mm and 25.00–50 mm were used. The first one was used to measure thickness while the second was used to measure the side length. Specific gloves were used while measuring the samples to reduce the transfer of temperature or any other kind of contamination from the hand. The amount of removed materials was calculated by the difference of samples before and after the WABF process. The thickness and side length were measured in 5 separate points in all samples as illustrated in Fig. 1(B). Material Removal Rate is calculated according to the Eq. (1)

$$MRR = \frac{Volume\ of\ Removerd\ material\ [mm^3]}{Process\ Time\ [min]} \quad (1)$$

The volume of removed material is calculated by the difference between the initial and final volumes (cross-section area multiplies by side) of the component.

2.4. Abrasive centrifugal barrel finishing

In this process, water, abrasive particulate (Fig. 2C) media and the components being polished are loaded in a container or barrel. This barrel rotates, and the rotational motion of the abrasive particles transitions to advanced flow, where some portions of the abrasive particles form an active layer as shown in Fig. 2(A and B). Depending on various factors such as geometry and quantity of abrasive particles, size and rotational speed of the centrifugal barrel, various types of flow can be obtained, which affect the MRR [25]. This process can also be performed without adding water and compound.

In this research, a commercial WACBF system (MFI HZ-40) as shown in Fig. 2(A and B) is used for finishing hexagonal LPBF samples. For stainless Steel and size of the samples, the Original Equipment Manufacturer (OEM) suggested two sizes of pyramid shape media comprising 3 × 3 and 6 × 6 mm. OEM also advised that rotational speed is an important factor in WACBF and time has an insignificant impact in roughness and this was approved by our primary experimentations. Therefore, four levels for rotational speed and two levels for media were selected. The control factors identified in the Taguchi L8 DOE (Table 1) were applied to quantify the effect on surface roughness and MRR. The used media for the finishing of the components was 3 × 3 and 6 × 6 ceramics with a pyramid in geometry (Equilateral triangle) from BV Products, which is shown in Fig. 2(C). The media with different sizes is recommended for general light and heavy deburring, fast and extra fast deburring and metal removal. Limited experimental data exists on the application of WACBF to AM production components, therefore WACBF process parameters were selected based on OEM recommendations.

2.5. Surface roughness measurement

2.5.1. Surface roughness measurement of the reference samples

WACBF surface roughness measurement was acquired with an optical profilometer (Alicona Infinite Focus) using 10X lens. Based on machining standards for surface roughness measurement, with a cut-off area of 10 × 3 mm, regions (consisting of approximately 6000 points) located in different areas of the manufactured specimens were measured. The normalized value of surface parameters was calculated

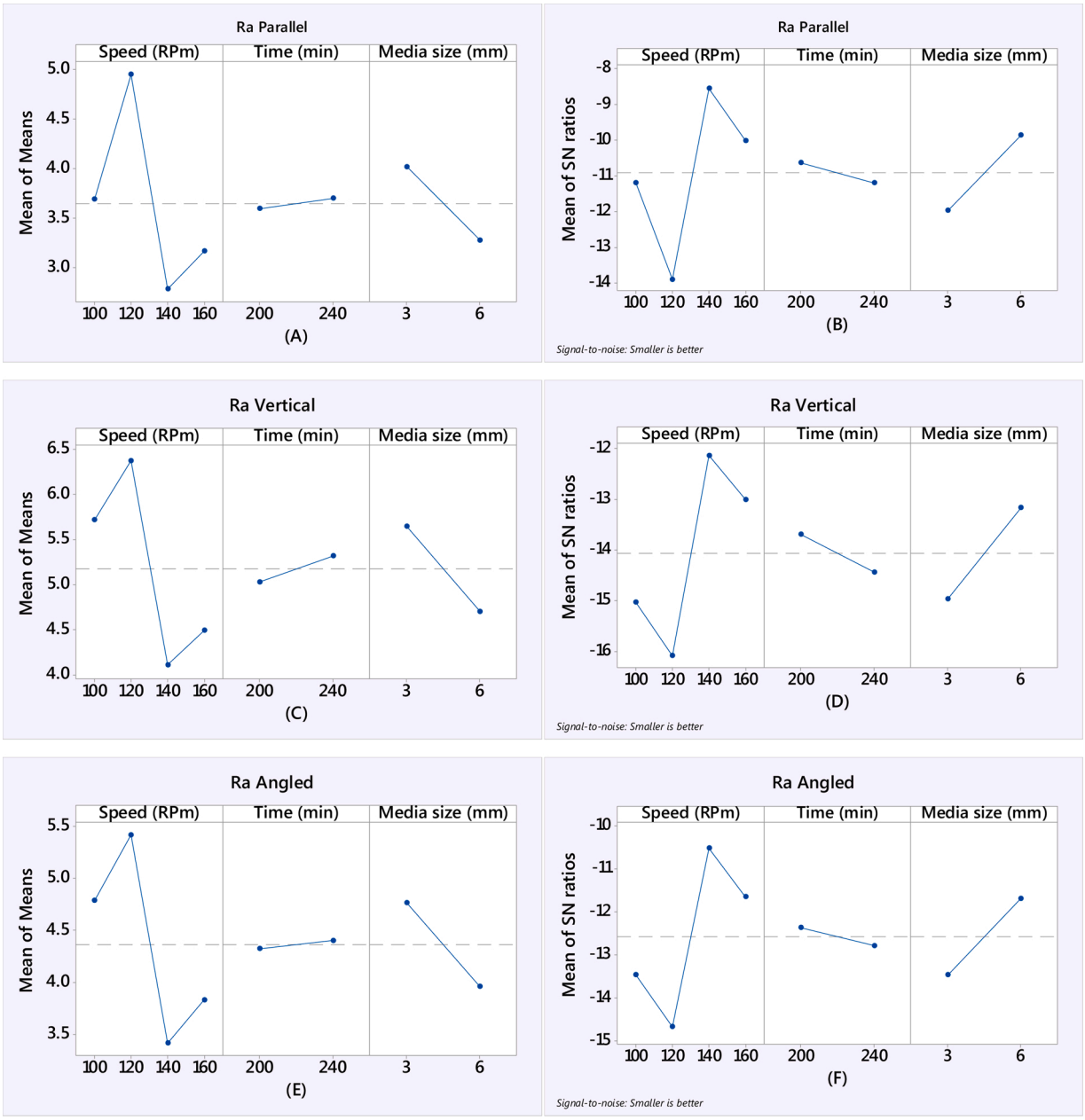

Fig. 3. SNR and mean effect analyze for roughness.

according to ISO 4288 and ISO 11,056 and a high pass built-in Gaussian filter was applied. The lateral and vertical resolutions of the profilometer were 10 nm and 400 nm. To ensure statistically robust outcomes, five different points of each experimental condition were measured. WACBF removes the material through the contact point of the media and workpiece so the removal area is the sum of the contact points. Therefore, different surface roughness can be obtained in different measurement directions. Also, surface roughness has a different trend in parallel, perpendicular and 45° to scan movement in LPBF parts; therefore, to assess the effect of WACBF in surface quality in a different direction, R_a was selected.

3. Results

3.1. Taguchi analysis and signal to noise (S/N) values for surface roughness

The results of the surface roughness measurement and materials removal rate for all three repetitions are presented in Tables A1–A3. Signal-to-noise Ratio (SNR) is the ratio of the measured outcome (surface roughness) to the associated noise (including measurement error and environmental effects) and is used to validate the accuracy of the obtained data. SNR is calculated based on the Taguchi equation [26,27]. In SNR analysis, horizontal lines indicate a reduced 'main effect' and lines of a higher slope are representative of the increased influence of changing parameters on observed outcomes. The objective is decreasing surface roughness; therefore, a Signal-to-noise (SN) criterion of 'smaller is better' was selected (Eq. 2). SNR and "Means" analyse robust the experiment when the minimum value of parameters including speed, time and media size in "Mean of Means" has the maximum values in "Mean of SNR". For R_a in parallel measurement, the minimum values in "Mean of Means" for speed, time and media size were obtained in 140 rpm, 200 min and 6 mm respectively (Fig. 3A). These points in "Means of SNR" Fig. 3(B) reached the maximum values, which shows the robustness of the experiment. Similar results were obtained for angled and vertical measurements in Fig. 3(C–F). Eq. 2 shows the SNR equation for

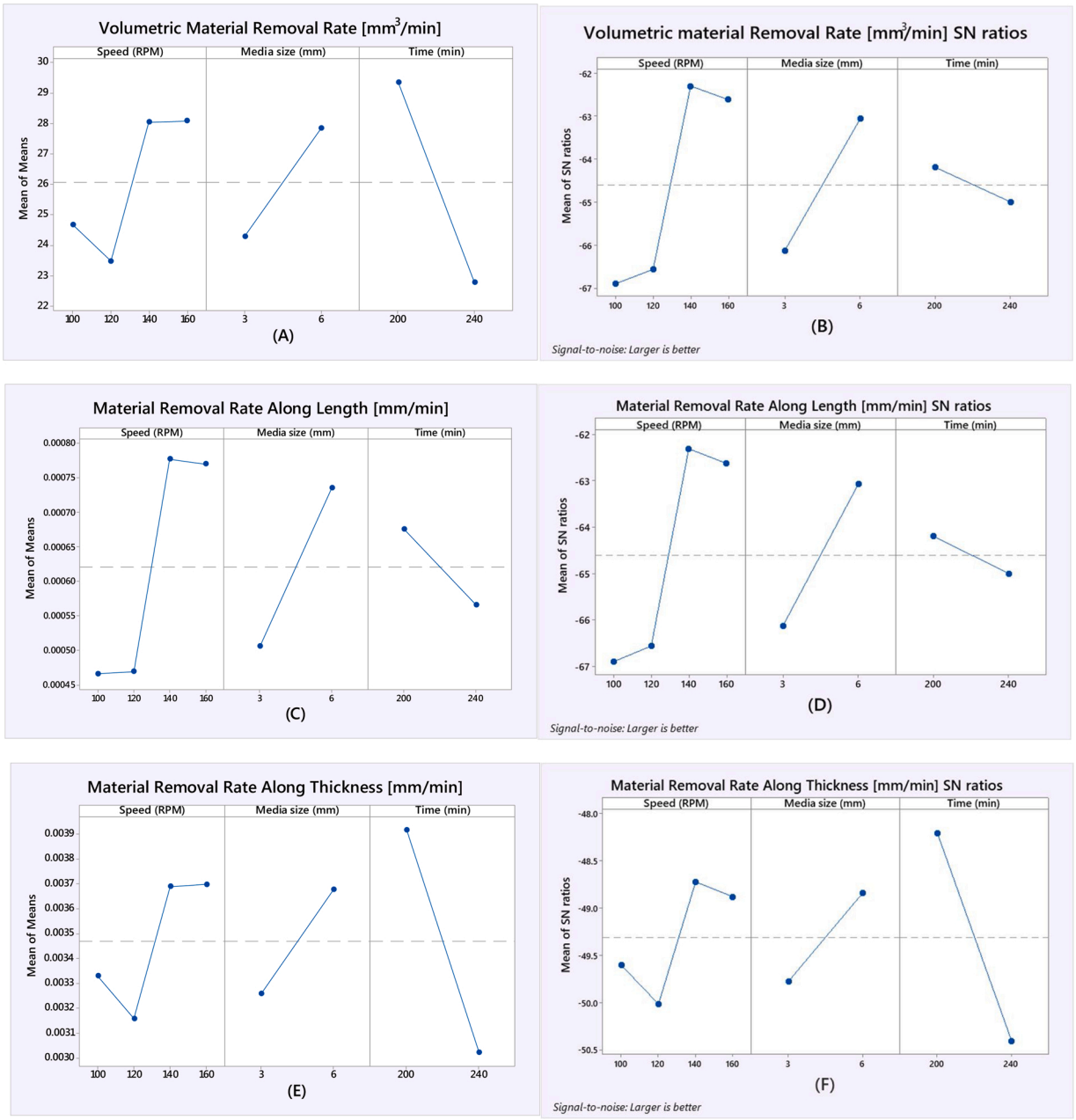

Fig. 4. SNR and mean effect analysis for MRR.

smaller is better criterion.

$$\frac{S}{N} = -10\left(\log_{10}\sum_{i=1}^{n}\frac{Y^2}{n}\right) \tag{2}$$

For MRR "larger is better" criterion was used so the highest and lowest points in SNR and "Mean of Means" diagrams have to be similar to show the robustness of the model. This shows the accuracy of the obtained data, thus proving no significant noise was observed (Fig. 4). Eq. 3 shows the SNR equation for larger is better criterion.

$$\frac{S}{N} = -10\left(\log_{10}\sum_{i=1}^{n}1\Big/\frac{Y^2}{n}\right) \tag{3}$$

3.2. The improvement of surface quality

A control specimen was manufactured and scanned for reference and to quantify the effect of WACBF on surface quality. The surface roughness of the reference samples for parallel, vertical and angled were obtained at 5.34 μm, 7.70 μm, and 6.33 μm respectively. The minimum values of the roughness obtained after WACBF were 2.01 μm, 3.3654 μm and 2.78 μm for parallel, vertical and angled measurements respectively. This shows that the WACBF process enhances the surface quality of as-built samples by 56.08 %, 56.33 % and 62.30 % for angled, vertical and parallel measurements. This outcome confirms uniform finishing and proves that WACBF is suitable for finishing of AM components.

3.3. MANOVA

Multivariate analysis of variance (MANOVA) is a statistical study to compare the multivariate average of results [28]. This method is used

Table 3
P-Values from a statistical test for MANOVA.

	Ra Parallel			Ra Vertical		
	Speed	Time	Media size	Speed	Time	Media size
P-Value	0.000	0.533	0.001	0.000	0.161	0.001
	Ra Angled			MRRv		
	Speed	Time	Media size	Speed	Time	Media size
P-Value	0.000	0.638	0.001	0.374	0.064	0.179

Table 4
Variables and ranges.

Process parameters	Variation range	Symbol	Variable
Speed (RPM)	100–160 (RPM)	X1	Input
Time (min)	200 – 240 (min)	X2	Input
Media size (mm)	3–6 (mm)	X3	Input
R_a parallel (μm)	–	Y1	Output
R_a vertical (μm)	–	Y2	Output
R_a angled (μm)	–	Y3	Output
Volumetric MRR		Y4	Output

when more than one dependent variable affects the outcomes. In an MANOVA, statistical differences on one continuous dependent variable by an independent grouping variable was examined. The results of MANOVA essentially tests whether or not the independent grouping variable simultaneously explains a statistically significant amount of variance in the dependent variable [29,30]. This method has four conditions: (I) output must be numerical, (II) output distribution must be normalized, (III) variances must physically exist and (IV) results have to be independent. Our study and results meet all conditions so MANOVA can be used to analyze the results.

The significance of the obtained results in relation to the null hypothesis is explained by P-Values. The null hypothesis shows that there is no relationship between every two variables being studied (one variable does not affect the other). It states how each variable significantly affects the results in terms of supporting the idea being investigated. The level of statistical significance is expressed as a P-value between 0 and 1. In MANOVA the smaller the p-value, the stronger the evidence to reject the null hypothesis. Commonly $P \leq 0.05$ is statistically significant and states strong evidence against the null hypothesis, as there is less than a 5% probability the null is correct. The P-value analysis has been carried out and the results based on Wilks criterion are listed in Table 3.

According to the results, speed and media size found to have P-Values≤0.5 therefore the null hypothesis is rejected. This shows these two variables are significant on the variation of roughness and MRR for both thickness and length. The results of MANOVA confirm that processing time has a negligible effect on the roughness values due to P-Values>.0.05 and accepting the null hypothesis. Therefore, surface roughness is not improved significantly by increasing processing time (higher than optimal value). However, for MRRv the only significant factor is the time of the process and media size and speed do not significantly change the MRR.

4. Discussions

Poisson regression was chosen to study the relation of speed, time and media size on surface roughness in all directions and robust the calculations and results. Two different regression models are calculated, including (I) the first power of variables and the interactions of variables and (II) the exponential of the first model. The performance of each method is compared with the coefficient of determination.

4.1. Poisson regression

Poisson regression is obtained through an exponential relation between input and output data. Table 4 shows control factors for the Poisson regression model.

Table 5
Poisson regression equations for various measurements.

Poisson regression equation	R^2 (%)
$Y_1 = e^{(-71.5+1.75X_1+0.0127X_2-1.05X_3-0.0139X_1{}^2+0.0075X_1X_3+0.000035X_1{}^3)}$	99.67
$Y_2 = e^{(-46.9+1.17X_1+0.0097X_2-0.72X_3-0.0094X_1{}^2+0.005X_1X_3+0.000024X_1{}^3)}$	97.95
$Y_3 = e^{(-50.4+1.26X_1+0.0097X_2-0.8X_3-0.0101X_1{}^2+0.0056X_1X_3+0.000026X_1{}^3)}$	99.26
$Y_4 = e^{(19.3-\ 0.392X_1+\ 0.0045\ X_2+\ 0.018X_3+\ 0.00320X_1{}^2+-\ 0.000082X_1X_2-\ 0.000008X_1{}^3)}$	93.16

In this study, an exponential function was used to model the surface roughness in different directions and MRR as shown in Table 5. According to the mean value analysis, rotational speed has a high order (third power) and stronger effect compared to time and media size, which linearly affect the results surface roughness measurements. The mathematical form of the equation for surface roughness and MRRv is the first order of each parameter, the interaction of speed and media size, and higher order of speed. The high R^2 and the contour plot related to each model is another proof of the accuracy.

Table 5 shows that the coefficient of determination for all measured roughness and MRR was obtained above 93.16 %, proving the accuracy. According to Figs. 6–8 and Poisson regression equations, the fluctuation of roughness and MRR as a function of speed, time and media size is non-linear. By increasing the rotational speed, roughness increased, decreased and again increased. This trend is similar to the grinding process [31,32].

The speed of the abrasive process affects the cutting forces. In this experiment, when rotational speed was increased to 120 rpm, a rougher surface was obtained. This is due to scratches and curving of media tips that reduce the performance of abrasive media as shown in Fig. 5 (Colors show the curvature on the tip of the media and polished sample).

By increasing rotational speed to 140 RPM, surface quality is improved. Higher rotational speed reduces the interaction time of the abrasive media and surface of the samples, which leads to less erosion and breaking effect of the media tips, thus sharper tips improve the quality of the surface. This area is the optimum area of rotational speed (Fig. 3A-C-E).

Increasing the speed to 160 rpm decreases surface quality. This act increases the temperature of the cutting area, which results in softening and the cutting process has been carried out more easily. The centrifugal force is a function of speed so when the speed increases, higher forces are generated. The mentioned mechanisms produce deeper indentation and increase surface roughness [33,34]. Therefore, more scratches occur, which reduces the surface quality that is called over-processing. Fig. 3 (A, C, E) and Figs. 5–8(A and B) illustrate the mentioned trend. Fig. 5 (A–C) shows the breaking spots and the surface profile of the breaking point.

As seen in Figs. 6–8, larger media size decreases the roughness. This observation occurs as larger media size is observed to flow more readily in the abrasive suspension, leading to decreased roughness. Also, larger media has more inertia, resulting in greater pressure and increased MRR that leads to better surface finish [32]. Fig. 9 shows the surface of the bigger media has more scratch than the small media.

Using different media has no effect on the surface when the speed is over 140 rpm. The reason is a stronger effect of rotational speed on the surface roughness, which is in agreement with P-Value analysis in Table 3. The P-Values of zero for rotational speed shows that this factor is very effective on surface roughness.

Increasing process time leads to increased roughness, which is related to three main reasons: (I) increasing temperature, (II) groove and scratch on the media and (III) less effective contact between samples. Higher temperature leads to softening and in this case, the material is sensitive to force and deformation [35,36]. The tip of the media has a

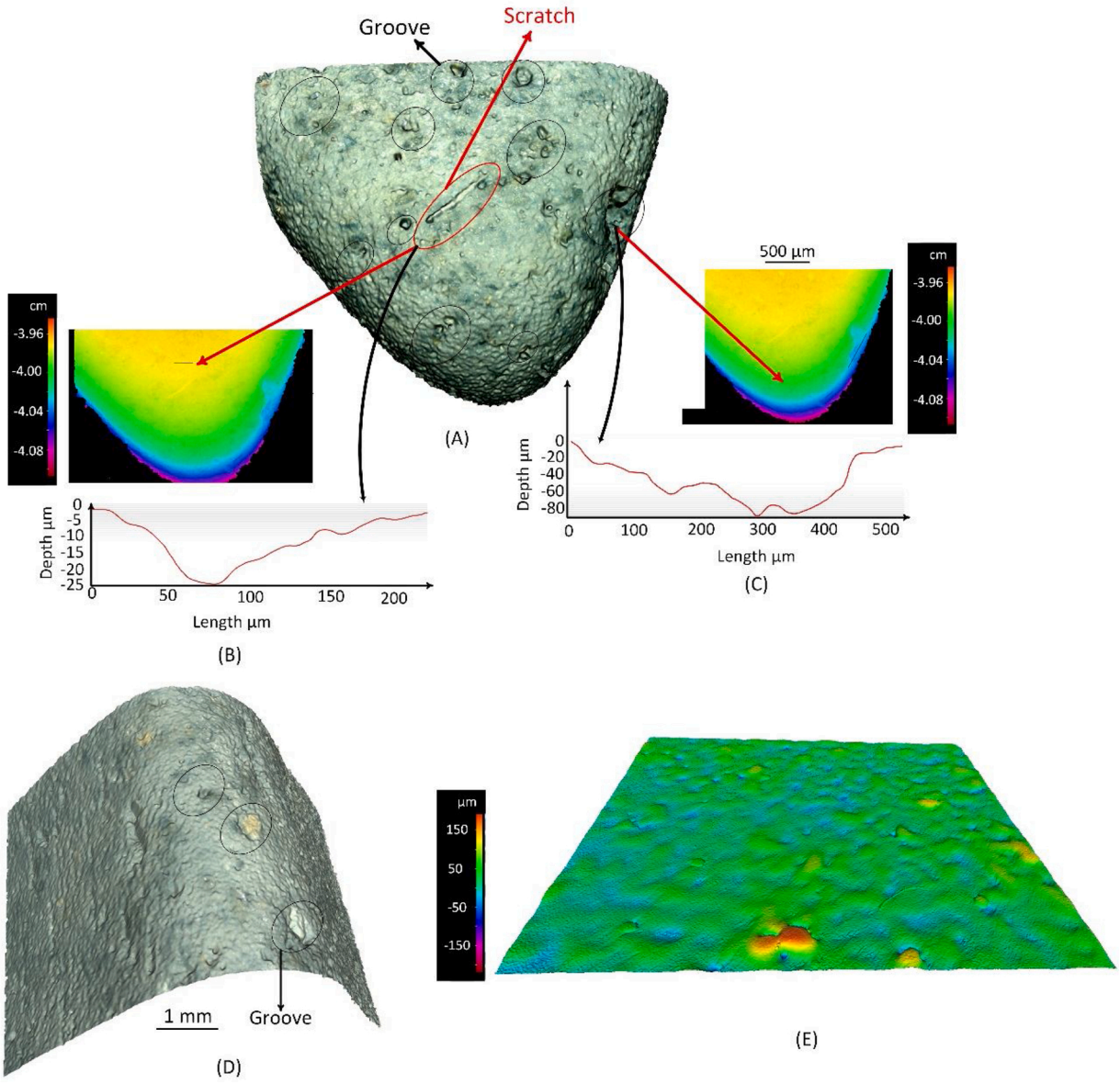

Fig. 5. (A-C) Scratch and curving on media tip for 160 rpm (D) Surface of the media for rotational speed 120 rpm (E) Polished samples.

very small contact area. Therefore, the pressure on the contact area of the samples increases radically, and more scratch and nonuniform material cutting occur [37,38].

In WACBF, MRR takes place from the surface peaks, thus producing the smooth surface, which is called micro-cutting. The surface of as-built LPBF components has sharp peaks related to the nature of the process, shown in Fig. 10(A). When the process runs for 200 min, all peaks removed away and good results are obtained (smooth surface), as shown in Fig. 10(B). However, by increasing the time of the process to 240 min due to impact or hitting effect of the media, the indentation depth increases and the surface becomes rougher [33,34].

The tips and edges of abrasive powder crystals are effective parameters on roughness. Thus, by increasing process time, the surface of the media erodes, which leads to a reduction of MRR and surface quality. In this occasion, more ineffective contacts between the samples and media occur and surface quality decreases [31,39].

Using bigger media leads to increase in the contact area and the reduction of volumetric material removal. By increasing the speed to 120 rpm, sharp edges of media scratch the component and small contact points are formed while the MRRv reduces. Increasing the process speed till 140 and 160 rpm reduces the interaction time between the media and the components (Fig. 11). Also, higher rotational speed increases the temperature of the process and due to thermal softening, higher penetration occurs and the MRRv increases. However, this mechanism reduces the surface quality as discussed in the previous sections. The interaction plots for volumetric material removal (Fig. 11) show that by increasing the time, the MRRv reduces. This is related to the media abrasion, losing sharp edges and subsequently sliding on the workpiece as shown in Fig. 5. Therefore, if the very fine surface quality is required, it is recommended to use the fresh media after each machining process.

5. Conclusions

This experiment quantifies the performance of WACBF as a surface enhancement process for LPBF stainless steel 316 L. This experiment provides statistically robust characterization of the WACBF process to enable commercial implementation of this enabling technology to overcome the poor surface roughness inherent in LPBF components. The following core observations are pertinent:

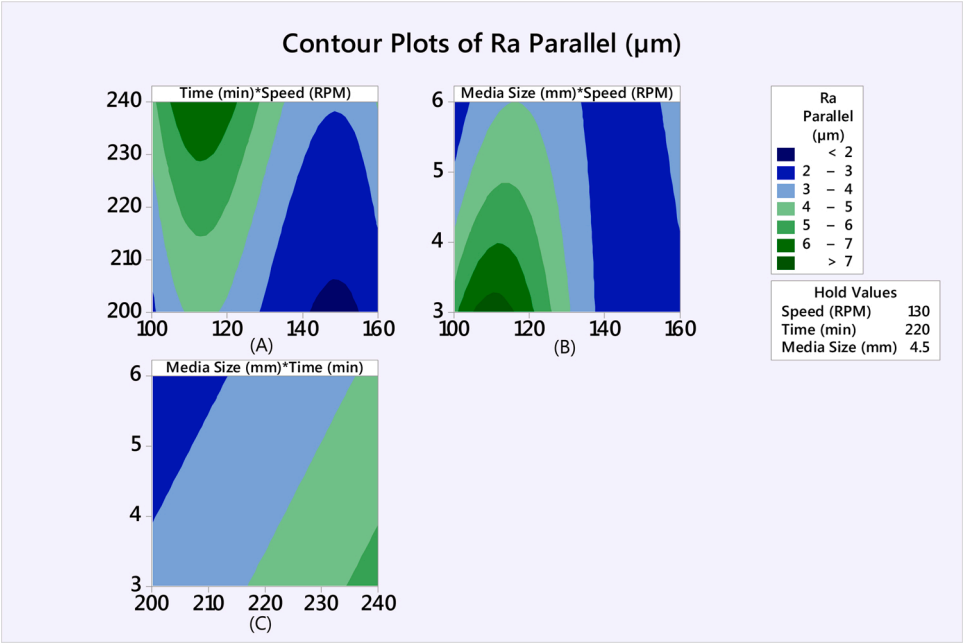

Fig. 6. Poisson regression for Parallel measurements.

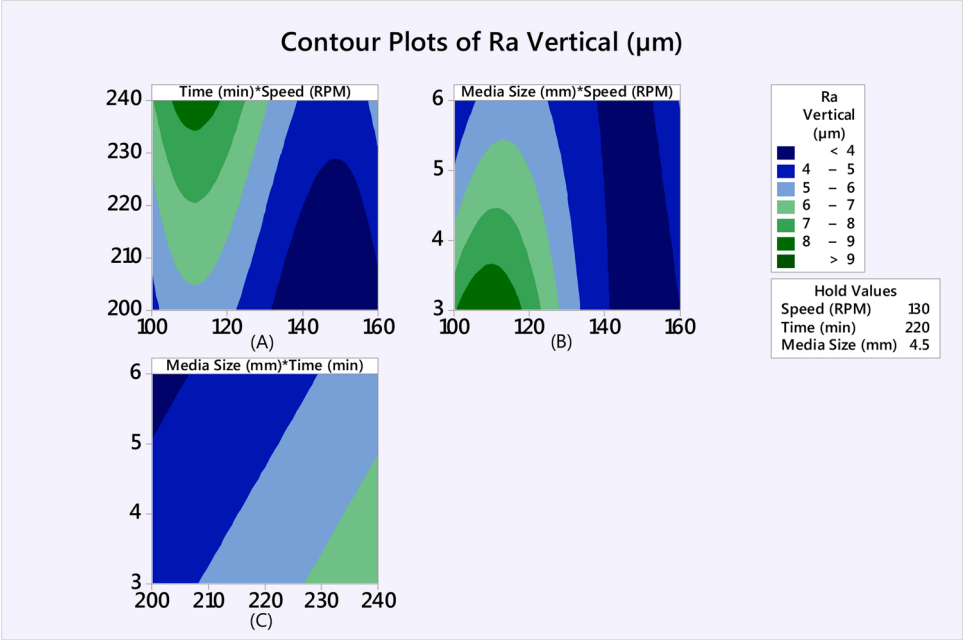

Fig. 7. Poisson regression for vertical measurements.

- Surface quality and MRR has non-linear behavior versus increasing the rotational speed. It is related to the removal of sharp edges of the media, thermal softening and lower interaction time between media and workpiece.
- Increasing the media size improves the surface quality and MRR, which is associated with easier flow of abrasive suspension including media and water. Moreover, bigger media has more mass, punching effect and inertia, so in the finishing process, it imposes more pressure and subsequently removes more materials, which in turn improves surface quality.
- Increasing the time of the WACBF increases the surface roughness that is associated with a higher temperature, decreasing the sharpness of the media and less effective contact.
- The best surface quality for all three measurements was obtained at the rotational speed of 140 rpm, media size of 6 mm and 200 min machining time.
- Results show that the WACBF improved the surface roughness of angled, vertical and parallel surfaces about 56.08 %, 56.33 %, and 62.30 % respectively. The results confirmed the uniform finishing and showed that WACBF is suitable for finishing of AM components.

The future work can be conducted to compare WACBF and ABF. Also, producing samples with different sizes and more complexity, such as lattice structure to shows the effect of WACBF process on the surface quality of internal and external surfaces can be another direction of future work.

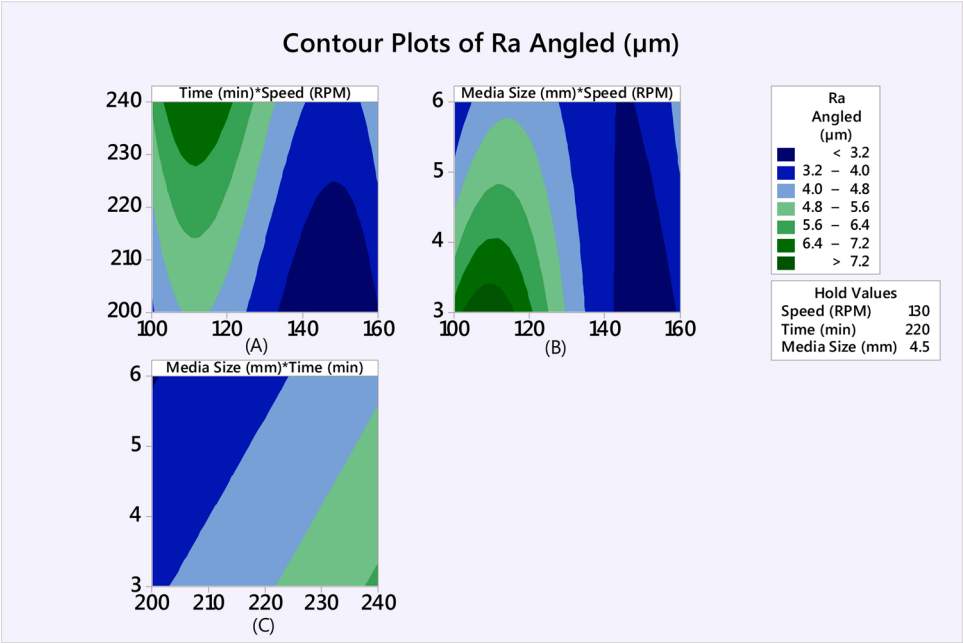

Fig. 8. Poisson regression for angled measurements.

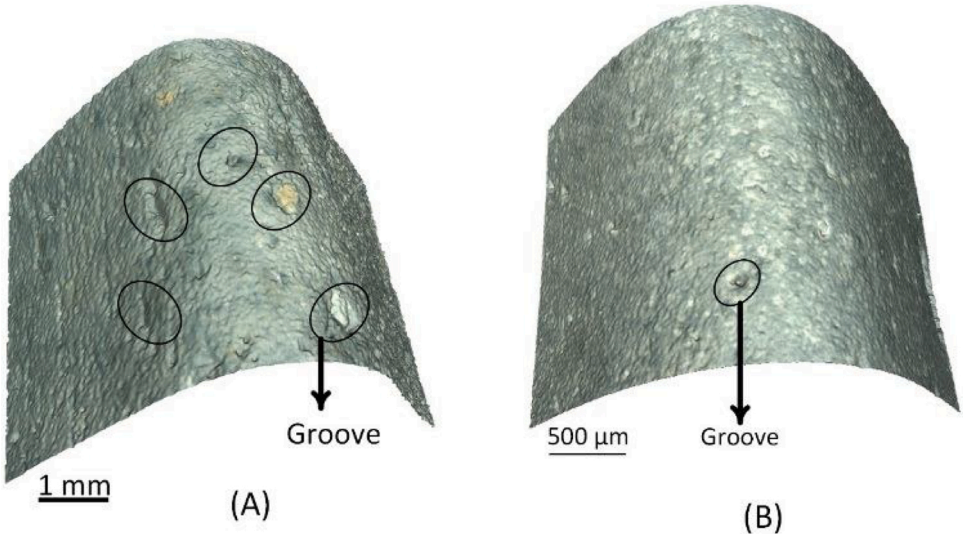

Fig. 9. Surface of (A) Big and (B) Small media.

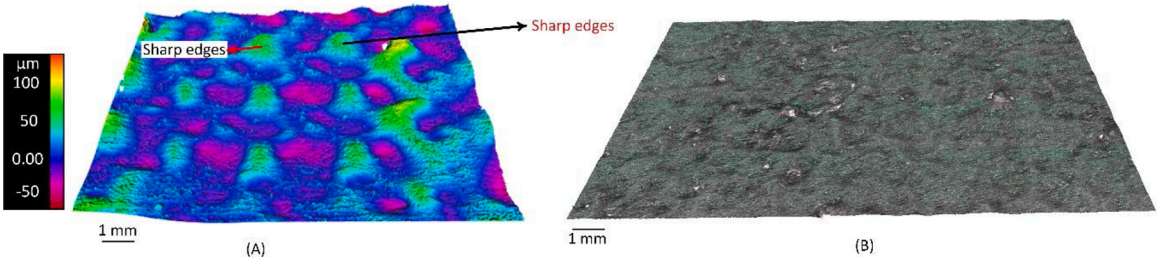

Fig. 10. (A) As-built surface (B) Surface after machining for test.

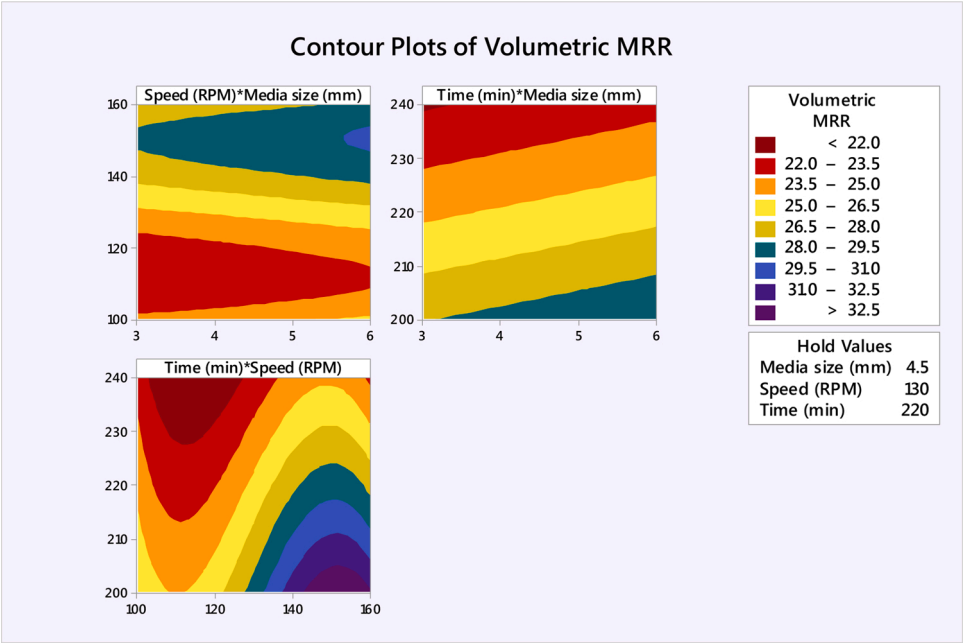

Fig. 11. Poisson regression for MRR.

Table A1
The results of roughness in different directions.

Ra Parallel	Re 1	Re 2	Re 3	Ra Vertical	Re 1	Re 2	Re 3	Ra Angled	Re 1	Re 2	Re 3
T1	4.348	4.369	4.415	**T1**	6.668	6.668	6.565	**T1**	5.592	5.626	5.681
T2	2.980	2.990	3.048	**T2**	4.806	4.812	4.782	**T2**	3.952	3.920	3.953
T3	4.865	4.925	4.918	**T3**	6.185	6.075	6.081	**T3**	5.275	5.302	5.316
T4	4.956	5.025	5.020	**T4**	6.678	6.652	6.580	**T4**	5.496	5.520	5.599
T5	2.012	2.016	2.011	**T5**	3.356	3.382	3.358	**T5**	2.755	2.832	2.754
T6	3.605	3.505	3.565	**T6**	4.910	4.825	4.832	**T6**	4.012	4.025	4.114
T7	3.115	3.056	3.117	**T7**	4.000	4.012	4.007	**T7**	3.600	3.605	3.541
T8	3.220	3.220	3.278	**T8**	4.896	4.889	5.162	**T8**	4.085	4.085	4.077

Re = Repetition, P = Parallel, V = Vertical, A = Angled.

Table A2
The results of the thickness measurement.

No	Re 1	Re 2	Re 3	No	Re 1	Re 2	Re 3	No	Re 1	Re 2	Re 3
T1	6.020	6.100	5.970	**T1**	6.020	6.050	6.110	**T1**	6.070	6.060	6.110
T2	6.040	6.080	6.060	**T2**	6.110	6.060	6.100	**T2**	6.100	6.140	6.090
T3	6.090	6.100	6.140	**T3**	6.170	6.130	6.150	**T3**	6.180	6.160	6.200
T4	6.050	6.070	6.030	**T4**	6.040	6.110	6.060	**T4**	6.030	6.030	6.180
T5	5.900	6.020	5.960	**T5**	5.960	5.940	6.040	**T5**	5.910	5.930	6.130
T6	6.030	6.030	5.970	**T6**	6.040	5.980	6.070	**T6**	6.030	6.000	6.090
T7	5.860	5.900	5.880	**T7**	5.870	5.900	5.900	**T7**	5.910	5.880	5.910
T8	6.050	6.030	6.040	**T8**	6.050	6.020	6.200	**T8**	6.150	6.190	6.170

Table A3
The results of the length measurement.

No	Re 1	Re 2	Re 3	No	Re 1	Re 2	Re 3	No	Re 1	Re 2	Re 3
T1	29.880	29.910	29.880	**T1**	29.880	29.980	29.900	**T1**	29.960	29.950	30.000
T2	29.800	29.790	29.900	**T2**	29.880	29.900	29.770	**T2**	29.800	29.850	30.020
T3	29.880	29.820	29.910	**T3**	29.880	29.900	29.920	**T3**	29.910	29.930	29.980
T4	29.880	29.850	29.850	**T4**	29.900	29.820	29.950	**T4**	29.880	29.880	29.940
T5	29.800	29.750	29.760	**T5**	29.810	29.790	29.770	**T5**	29.850	29.910	29.910
T6	29.800	29.780	29.880	**T6**	29.800	29.880	29.840	**T6**	29.810	29.890	29.880
T7	29.790	29.770	29.810	**T7**	29.740	29.780	29.880	**T7**	29.830	29.800	29.800
T8	29.900	29.830	29.820	**T8**	29.820	29.880	29.880	**T8**	29.830	29.830	29.980

Declaration of Competing Interest

The authors report no declarations of interest.

Appendix A

References

[1] Khorasani A, et al. The effect of SLM process parameters on density, hardness, tensile strength and surface quality of Ti-6Al-4V. Addit Manuf 2019;25:176–86.
[2] Miranda G, et al. A study on the production of thin-walled Ti6Al4V parts by selective laser melting. J Manuf Process 2019;39:346–55.
[3] Salman OO, et al. Impact of the scanning strategy on the mechanical behavior of 316L steel synthesized by selective laser melting. J Manuf Process 2019;45:255–61.
[4] Khorasani AM, et al. A comprehensive study on variability of relative density in selective laser melting of Ti-6Al-4V. Virtual Phys Prototyp 2019:1–11.
[5] Boschetto A, Bottini L. Manufacturability of non-assembly joints fabricated in AlSi10Mg by selective laser melting. J Manuf Process 2019;37:425–37.
[6] Carluccio D, et al. The influence of laser processing parameters on the densification and surface morphology of pure Fe and Fe-35Mn scaffolds produced by selective laser melting. J Manuf Process 2019;40:113–21.
[7] Khorasani AM, et al. An improved static model for tool deflection in machining of Ti–6Al–4V acetabular shell produced by selective laser melting. Measurement 2016;92:534–44.
[8] Khorasani AM, et al. A comprehensive study on surface quality in 5-axis milling of SLM Ti-6Al-4V spherical components. Int J Adv Manuf Technol 2018;94(9–12):3765–84.
[10] Löber L, et al. Comparison of different post processing technologies for SLM generated 316l steel parts. Rapid Prototyp J 2013;19(3):173–9.
[11] Rossi S, Deflorian F, Venturini F. Improvement of surface finishing and corrosion resistance of prototypes produced by direct metal laser sintering. J Mater Process Technol 2004;148(3):301–9.
[12] Beaucamp AT, et al. Finishing of additively manufactured titanium alloy by shape adaptive grinding (SAG). Surf Topogr Metrol Prop 2015;3(2). p. 024001.
[13] Lamikiz A, et al. Laser polishing of parts built up by selective laser sintering. Int J Mach Tools Manuf 2007;47(12–13):2040–50.
[14] Uno Y, et al. High-efficiency finishing process for metal mold by large-area electron beam irradiation. Precis Eng 2005;29(4):449–55.
[18] Boschetto A, et al. Post-processing of complex SLM parts by barrel finishing. Appl Sci 2020;10(4):1382.
[19] Nalli F, et al. Effect of industrial heat treatment and barrel finishing on the mechanical performance of Ti6Al4V processed by selective laser melting. Appl Sci 2020;10(7). p. 2280.
[20] Lesyk D, et al. Surface finishing of complexly shaped parts fabricated by selective laser melting. In: Grabchenko's International Conference on Advanced Manufacturing Processes; 2019.
[21] Lesyk D, et al. Post-processing of the Inconel 718 alloy parts fabricated by selective laser melting: effects of mechanical surface treatments on surface topography, porosity, hardness and residual stress. Surf Coat Technol 2020;381:125136.
[22] Na W, et al. Experiment and simulation analysis on the mechanism of the spindle barrel finishing. Int J Adv Manuf Technol 2020:1–18.
[23] Singh G, et al. Effects of chemically assisted magnetic abrasive finishing process parameters on material removal of inconel 625 tubes. Procedia Manuf 2020;48:466–73.
[24] Ferchow J, et al. Model of surface roughness and material removal using abrasive flow machining of selective laser melted channels. Rapid Prototyp J 2020.
[25] Boschetto A, Bottini L, Veniali F. Microremoval modeling of surface roughness in barrel finishing. Int J Adv Manuf Technol 2013;69(9–12):2343–54.
[26] Box G. Signal-to-noise ratios, performance criteria, and transformations. J Technomet 1988;30(1):1–17.
[27] Srivastava M, Rathee S. Optimisation of FDM process parameters by Taguchi method for imparting customised properties to components. Virtual Phys Prototyp 2018;13(3):203–10.
[28] Fatemi S, et al. Experimental investigation of process parameters on layer thickness and density in direct metal laser sintering: a response surface methodology approach. Virtual Phys Prototyp 2017;12(2):133–40.
[29] Warne RT. A primer on multivariate analysis of variance (MANOVA) for behavioral scientists. Prac Assess Res Eval 2014:19.
[30] Stevens J. Applied multivariate statistics for the social sciences. Mahwah, NJ: Lawrence Erlbaum; 2002. p. 510–1.
[31] Khorasani AM, et al. Production processes: an introduction of metal forming and metal cutting. 2009.
[32] Khorasani AM, Khavanin Zadeh MR, Vahdat Azad A. Advanced production processes. Psychology, art and technology; 2012. p. 207.
[33] Sankar MR, Jain V, Ramkumar J. Rotational abrasive flow finishing (R-AFF) process and its effects on finished surface topography. Int J Mach Tools Manuf 2010;50(7):637–50.
[34] Reddy MK, Sharma A, Kumar P. Some aspects of centrifugal force assisted abrasive flow machining of 2014 Al alloy. Proc Inst Mech Eng Part B J Eng Manuf 2008;222(7):773–83.
[35] Astakhov VP, Joksch S. Metalworking fluids (MWFs) for cutting and grinding: fundamentals and recent advances. Elsevier; 2012.
[36] Byers JP. Metalworking fluids. crc Press; 2016.
[37] Jackson MJ, Davim JP. Machining with abrasives. Springer; 2011.
[38] Shaw MC. Principles of abrasive processing (Oxford series on advanced manufacturing). 1996.
[39] Malkin S, Guo C. Grinding technology: theory and application of machining with abrasives. Industrial Press Inc.; 2008.